ELSEVIER

Polymer 44 (2003) 2081–2090

polymer

www.elsevier.com/locate/polymer

Effects of perfluoroether concentration and curing protocol on morphology and mechanical properties of toughened TGDDM/MNA resin systems

G. Ragosta[a], P. Musto[a], G. Scarinzi[a], L. Mascia[b,*]

[a]*Institute for Research and Technology of Polymers, CNR, Comprensorio Olivetti, Bdg. 70, 80078 Pozzuoli, Napoli, Italy*
[b]*Institute of Polymer Technology and Materials Engineering, Loughborough University, Leicestershire, Loughborough LE11 3QL, UK*

Abstract

Previous published work has shown that hydroxyl terminated perfluoroether oligomers can be suitably modified and functionalised to make them miscible with epoxy resins in the uncured state. The reaction conditions can adjusted to induce phase separation either through spinodal decomposition to produce an IPN type morphology, or by nucleation and growth if a dispersed-particle microstructure is required.

In the present work we examine the relative toughening enhancement efficiency of the two possible heterophase morphologies. Both systems show a sigmoidal increase in fracture toughness, with increasing concentration of the perfluoroether modifier. However, this takes place at much lower modifier concentrations for the systems with a particulate morphology (about 3.5% w/w) than for IPN systems (about 7.5% w/w). The maximum fracture toughness achievable for the two systems, on the other hand, is very similar and coincides with the concentration at which co-continuous phases are formed.

These differences in morphology, however, are not reflected in the variation of modulus and compressive yield strength with increasing concentration of perfluoroether modifier, in so far as both systems exhibit a gradual and small reduction in property with increasing concentration. Furthermore, the dynamic mechanical spectra of the two systems are very different, but the changes resulting from increasing the concentration of toughening agent are relatively small in either case.

Nanoindentation tests indicate that it is the local plasticity, brought about by the presence of the softer perfluoroether phase, which is responsible for the enhancement of fracture toughness. This is corroborated by AFM examinations, which reveal local plastic deformations in the regions surrounding the softer particles.

Keywords: Epoxy resin; Perfluoroethers; Toughening agents

1. Introduction

Telechelic extended perfluoroether oligomers have been previously studied as toughening agents for epoxy resins, particularly for difunctional systems, such as diglycidylether of bisphenol-A (DGEBA) [1,2].

These-acid functionalised oligomeric modifiers have been selected primarily for their inherent high thermal oxidative degradation resistance, in order to provide a viable alternative to carboxyl-terminated butadiene acrylonitrile oligomers (CTBN) for applications at elevated temperatures [3].

They are produced by reacting an hydroxyl-terminated perfluoroether oligomer first with chlorendic anhydride and then with caprolactone in molar amounts to produce approximately unitary telechelic extensions terminated by carboxylic acid groups [1].

More recently these oligomers have also been used in tetraglycidyl diamino diphenyl methane (TGDDM) resins systems, but only as miscibilised systems cured by a one-step schedule to produce IPN morphologies [3,4].

Efficient toughening of rigid polymers, particularly network polymers, relies on the precipitation of the oligomeric modifier as rubbery, or soft, inclusions through a nucleation and growth mechanism [5,6]. It has often been found that highly miscible systems do not undergo this type of phase separation during curing and, therefore, will not provide a very efficient toughening mechanism, particularly for tetrafunctional epoxy systems. These deductions were made from studies on the use of polysiloxanes and aromatic polymeric modifiers [7,8]. Both systems were selected for their intrinsic

* Corresponding author. Tel.: +44-1509-223339; fax: +44-1509-234516.
E-mail address: l.mascia@lboro.ac.uk (L. Mascia).

0032-3861/03/$ - see front matter © 2003 Elsevier Science Ltd. All rights reserved.
doi:10.1016/S0032-3861(03)00060-0

resistance to thermal oxidation. A particle precipitation mechanism by nucleation and growth was achieved with the use of low molecular weight block copolymers containing resin-soluble end blocks.

Earlier searches for thermally stable modifiers capable of undergoing phase separation by nucleation and growth were based on block copolymers containing central crystallisable-segments, such as poly(ether ether ketone) or poly(butylene terephthalate), and resin-soluble amorphous end blocks based on poly(ether sulphone) and poly(etherimide) [9,10].

Once more these were not found to be particularly effective in achieving the desired mechanism for phase separation despite the driving force provided by the crystallisation tendency of the central blocks. High concentrations of the modifier were necessary to enable the modifier to crystallise in order to induce phase separation.

In contrast to these systems the perfluoroligomer based modifiers were found to induce phase separate very easily even at low concentrations, without any sign of plasticisation, as evidenced by the largely unaffected T_g of the resulting cross-linked system [1,2].

The curing protocol could be adjusted to produce either a co-continuous morphology, containing nanostructured domains, or micron-sized precipitated particles system, consisting of very small aggregated primary particles. The latter systems were found to be effective in increasing the toughness of bifunctional DGEBA epoxy resins even at low concentrations.

In our previous work we have shown that these modified perfluoroethers would also separate as co-continuous nanostructured domains in mixtures with tetrafunctional epoxy resins, TGDDM, but required fairly high levels of additions to achieve an appreciable increase in toughness [3].

In the present paper, we examine the possibility of inducing phase separation with particle precipitation and compare the efficiency of the two types of morphologies for toughness enhancement of tetrafunctional epoxy resins.

2. Experimental

2.1. Materials

The epoxy resin was a commercial grade of tetraglycidyl 4-4′-diaminodiphenyl-methane (TGDDM) supplied by Ciba-Geigy. The hardner was methyl-bicyclo-(2,2,1)-heptene-3,3 dicarboxylic acid anhydride (methyl nadic anhydride, MNA, obtained from Fluka). Benzyl dimethylaniline (BDMA, supplied by Aldrich) was used as an accelerator. The chemical modification and carboxyl functionalisation reactions for the hydroxyl terminated perfluoroether oligomer (PFO) have been described elsewhere [1].

The chemical structure of the resin components used is shown below:

(a) TGDDM—tetraglycidyl-4-4′ diaminodiphenyl-methane

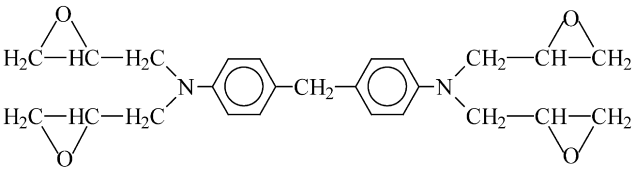

(b) MNA—methylbicyclo-(2,2,1)-heptene-2,3 dicarboxylic acid anhydride

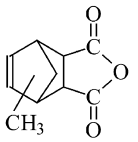

(c) PFO—carboxyl-terminated perfluoroether pre-polymer, a 1:1 mixture of

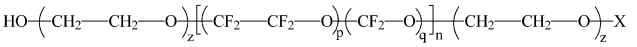

and

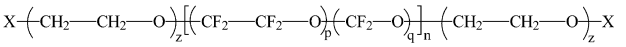

where

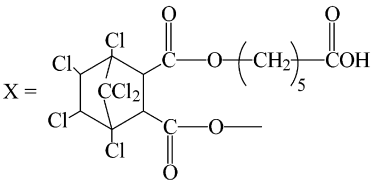

$z = 1.5$; p/q molar ratio $= 0.67$ and $n \cong 10$.

2.2. Preparation of a typical resin mixture

(a) *Particle dispersed systems*. For the preparation of mixtures yielding a particle dispersed morphology in the final cured products, TGDDM was first reacted with different amounts of PFO in the presence of triphenylphosphine (TPP) catalyst (1.0 wt% with respect to TGDDM) at 100 °C for 6 h in a glass flask, under vigorous mechanical stirring, to produce an epoxy-extended prepolymer dissolved in excess TGDDM resin. After cooling down to 80 °C, MNA hardener (30.3 g) and BDMA (0.25 g) were added.

(b) *IPN systems*. For systems exhibiting an IPN morphology in the final cured product the three resins components, TGDDM, PFO and MNA, were mixed together in the specified order without prereacting the perfluoroether with the epoxy resin.

In both cases the resin mixture was stirred for 10 min after the addition of the BDMA accelerator and then poured into a glass mould to produce plaques about $150 \times 150 \times 3$ mm^3. These were subsequently heated for 12 h at 120 °C and post-cured for 3 h at 150 °C and 1 h at 180 °C. This curing protocol produced visually transparent plaques for all IPN systems and opaque samples for PFO concentrations up to about 7.0 wt% for the particle-dispersed systems. At higher PFO content, the samples were visually transparent and indistinguishable from those obtained with the pre-reaction protocol.

The weight ratio of epoxy to anhydride components has been kept constant at 100/80, which corresponds to a 2:1 molar ratio.

2.3. Mechanical tests

Mechanical tests were performed at room temperature using an Instron instrument, model 4505, operating at a clamp separation speed of 1 mm/min in all cases. The modulus of the cured resins was measured from tests carried out in a flexural mode from the tangent of the force/extension curve, using rectangular specimens, $60.0 \times 6.0 \times 4.0$ mm^3, and a span/width ratio of 8:1. The yield strength was measured in compression on specimens, $60.0 \times 6.0 \times 4.0$ mm^3, loaded along the length.

Due to the absence of a definite maximum in the load/contraction curves the yield strength was estimated as the stress corresponding to the 5% offset strain from the elastic strain.

Fracture toughness was assessed using a multiple crack length procedure on V-notched rectangular specimens, $60.0 \times 6.0 \times 4.0$ mm^3, SEN types with notch length varying from, 1.5 to 4.5 mm, extended by 0.2 mm by a razor blade fixed to a micrometer apparatus. The actual length of the notch was measured using an optical microscope after fracturing the specimens.

The critical stress intensity factor, K_c (which corresponds to the K_{IC} value) was calculated from the slope of the plot of stress to at fracture propagation against $1/a^{1/2}$, as shown in Fig. 1, which is based on the equation $K_c = Y\sigma\sqrt{a}$, where the stress σ was calculated as the outer skin stress for a rectangular beam in 3-point bending, Y is the compliance calibration factor obtained from tables quoted in the literature [11] and a is the notch length.

The critical strain energy release rate, G_c, was estimated from the slope of the plot of the elastic energy at fracture initiation (U) recorded at each crack length from the area under the load–deflection curve, against the product $BW\phi$, where B and W are the thickness and the width of the specimen, respectively, and ϕ is a correction factor that takes into account the rate of change of compliance (C) with

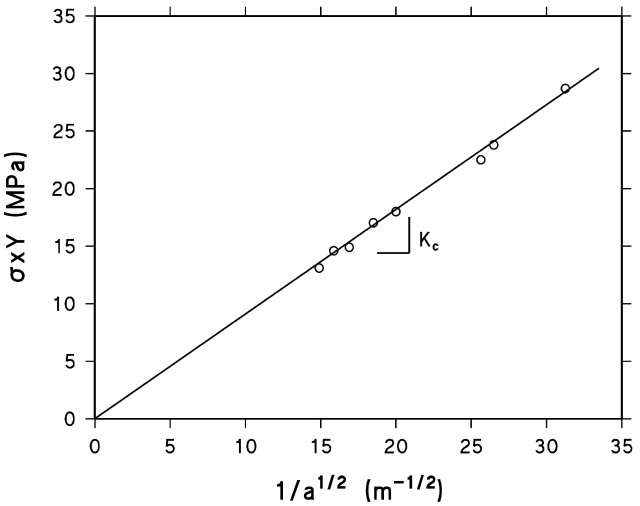

Fig. 1. Typical plot of load to fracture against square root of reciprocal crack length.

crack length,

$$\phi = C\left[\frac{dC}{d\left(\frac{a}{W}\right)}\right]^{-1}$$

using the equation

$$G_c = \frac{U}{BW\phi}$$

The values of ϕ were obtained from the tables reported in the literature [12].

2.4. Morphological examinations

The morphology of the samples was examined on fractured specimens by SEM, using a Philips instrument model XL20 and by AFM on a TA Instruments 2990 Micro-Thermal Analyzer equipped with a TM Microscopes Explorer. The type of probe used, was the TM Microscopes 1660-00 silicon low resonance frequency unit. This has a resonance frequency in the range 160–220 kHz and a nominal force constant of 48 N m^{-1}. The operating method employed was intermittent contact mode, simultaneously producing topographic and mechanical property-based images.

From the printed micrographs of the SEM examinations an image analyser was used to determine the particle size and particle size distribution of in systems with a particle-dispersed microstructure.

2.5. Dynamic mechanical tests

Dynamic mechanical spectra for the various samples were obtained from measurements of the loss modulus over a wide range of temperatures. The apparatus used was a TA Instrument, model 2980, operating as simple cantilever with

a load applied at 17 mm distance from the clamp. Oscillations were applied with amplitude of 20 μm and a frequency of 1 Hz. and the temperature was scanned at 5 K per minute.

2.6. Nanoindentation measurements

The instrument used for the hardness measurements was a Nanotest 600 manufactured by Micromaterials. A Bercovich type indentor with a 65.3° phase angle was used to a depth of penetration of 4 μm, requiring a load in the region of 90 mN, applied over a period of one minute before the readings were taken. The surface of the samples was polished with diamond pads to eliminate possible errors from surface irregularities.

An area of 2×2 mm^2 was scanned for samples with a particle-dispersed morphology, taking readings at 200 μm intervals, giving a total of 100 measurements per sample.

For the control samples 10 readings were taken, whereas for those with an IPN morphology a total of 30 measurements were made, probing the sample at 200 μm distance. In all cases the extent of unrecovered (plastic) deformation was also measured upon removal of the applied load.

3. Results and discussion

3.1. Modulus, yield strength and nanoindentation measurements

The variation of flexural modulus and yield strength with concentration of modified perfluoroether (PFO) for both types of morphology is shown in Fig. 2(i) and (ii). Although the decrease in modulus and yield stress with increasing concentration of the fluoroligomer was entirely predictable, the remarkable similarity of the deformational behaviour of the IPN and the particle-dispersed systems, at equal concentration of PFO, cannot be readily explained. In any case, it is worth noting that the maximum reduction observed for these properties is quite small, approximately 10% for the modulus and 15% for the yield strength, suggesting that the properties of the two constituent phases for both systems cannot be vastly different. This is confirmed by the hardness data obtained from the nanoindentation measurements, see Tables 1 and 2.

3.2. Fracture behaviour and morphological examinations

The variation of the critical stress intensity factor, K_c, and critical strain energy release rate, G_c, as functions of the PFO content of the epoxy resin mixture, is shown in Fig. 3(i) and (ii). From these it can be seen that both K_c and G_c increase rapidly upon reaching a critical concentration of PFO modifier and subsequently reach a plateau. It is to be remarked, however, that the rapid change occurs at much

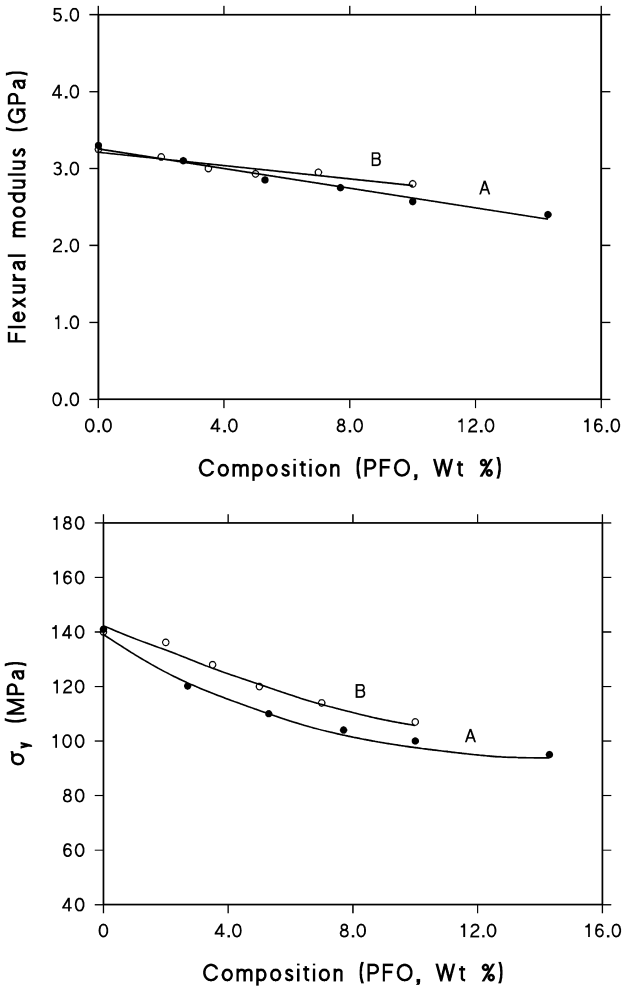

Fig. 2. (i) Plot of flexural modulus against fluoroligomer content in the resin: (A) IPN systems; (B) particle-dispersed systems. (ii) Plot of compressive yield stress against fluoroligomer content: (A) IPN systems; (B) particle-dispersed systems.

lower PFO concentrations for systems with particle-dispersed microstructures than those with IPN morphologies. It is worth emphasising also that the toughening effect resulting from the presence of the PFO containing phase is much more pronounced when the fracture data are expressed in terms of G_c values. In particular, the data in Fig. 4 show that at PFO concentrations where the fracture toughness reaches the plateau level, the value of G_c increases by a factor of about 5 with respect to the control resin system, whereas the increases in K_c are about half this amount. These improvements in toughness, in any case, are

Table 1
Hardness values (MPa) of samples with an IPN morphology

Sample type wt% PFO	Number of readings	Hardness value (average)	Standard deviation
0	10	325	1
7.5	20	306	1
10.0	10	261	2

Table 2
Hardness values (MPa) of samples formulated and thermally treated to obtain a particle-dispersed morphology

Sample type wt% PFO	Number of readings equal to or less than 280	Hardness value (average)		Standard deviation
		Rigid phase	Soft phase	
0	0	325	N/A	1
2.0	3	337	280	4
3.5	14	327	254	7
7.0	18	335	232	15
10.0	100	271	271	2

comparable with those reported for epoxy resins toughened with functionalised polysulphones or polyetherimides [9,10], but the concentrations required are much lower for PFO based modifiers.

Typical SEM micrographs of the fracture surface of specimens from fracture toughness tests, taken near the crack tip, are shown in Figs. 4 and 5. For the control resin (Fig. 4(i)), the surface appears very smooth, showing very little sign of plastic deformations ahead the crack tip during fracture propagation. Noticeable signs of localised plastic deformations are visible, on the other hand, on the fractured surfaces of the PFO modified samples. In all cases, at concentrations of fluoroligomer higher than 7.0 wt% there are no visible signs of particle formation, as shown by the micrograph in Fig. 4(ii), and the morphology appears to be very similar to that reported previously for IPN systems [3]. For the latter it was shown that the PFO containing domains were in the region of 3–10 nm.

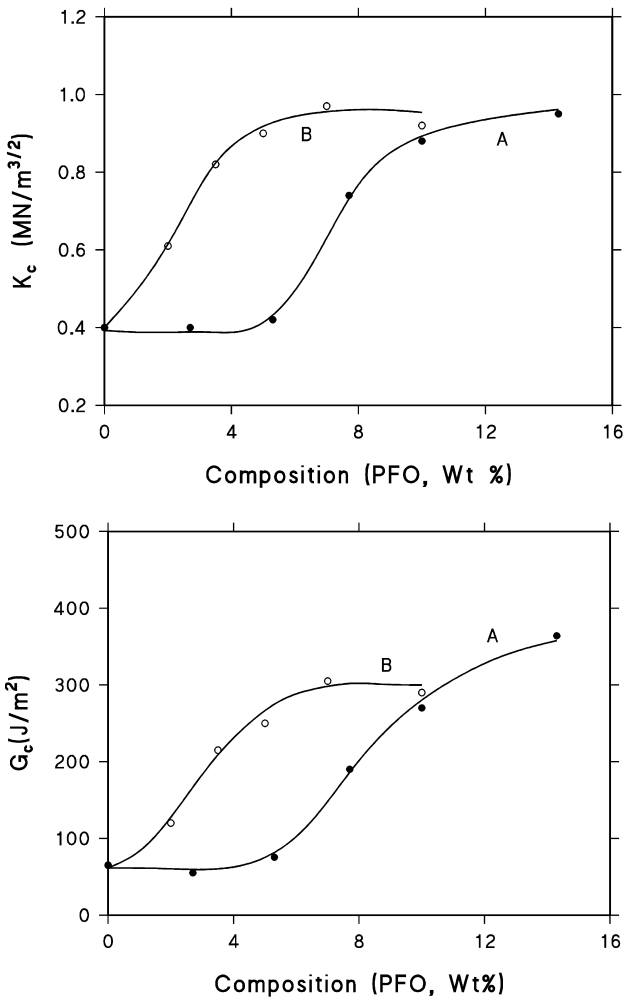

Fig. 3. (i) Variation of the critical stress intensity factor, K_c, with increasing fluoroligomer content in the resin: (A) IPN systems; (B) particle-dispersed systems. (ii) Variation of critical strain energy release rate, G_c, with increasing fluoroligomer content in the resin: (A) IPN systems; (B) particle-dispersed systems.

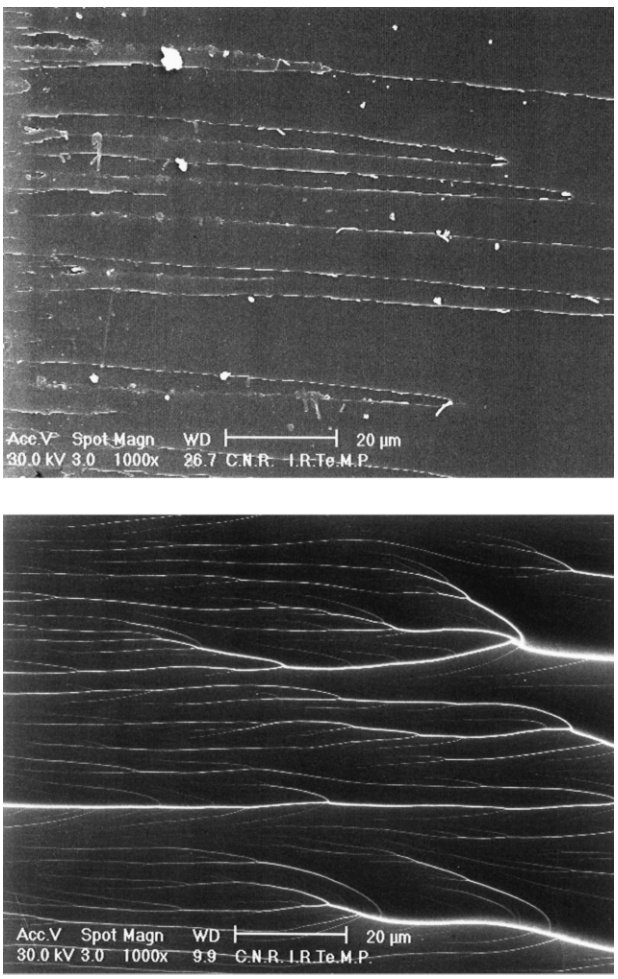

Fig. 4. (i) SEM micrograph of the fractured surface of the base epoxy resin. (ii) SEM micrograph of the fractured surface of epoxy resin containing 14.0 wt% PFO prepared as for particle precipitated systems.

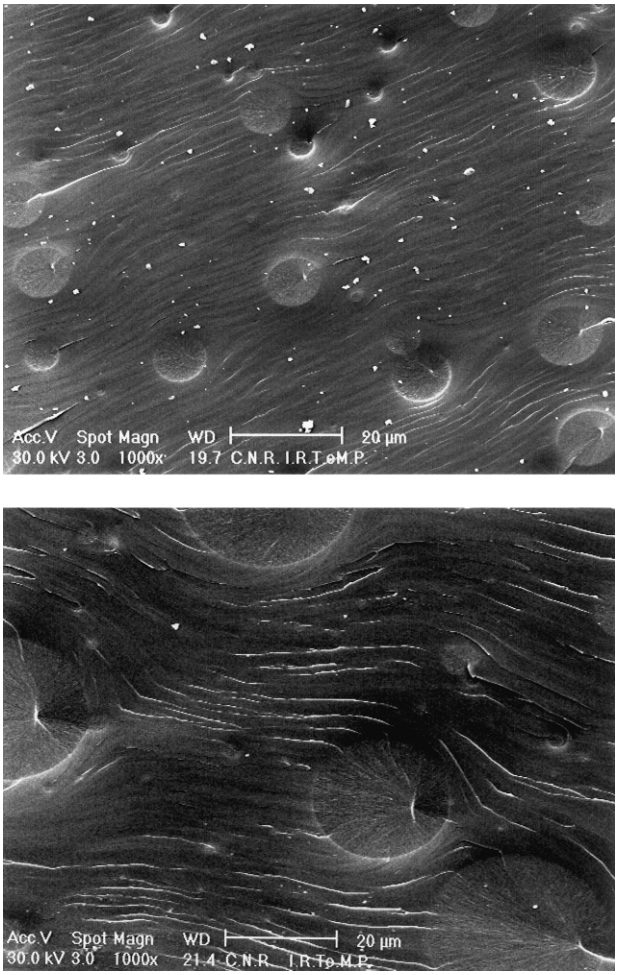

Fig. 5. (i) SEM micrographs of fractured surfaces of particle dispersed systems: containing 3.5 wt% PFO. (ii) SEM micrographs of fractured surfaces of particle dispersed systems: containing 7.0 wt% PFO.

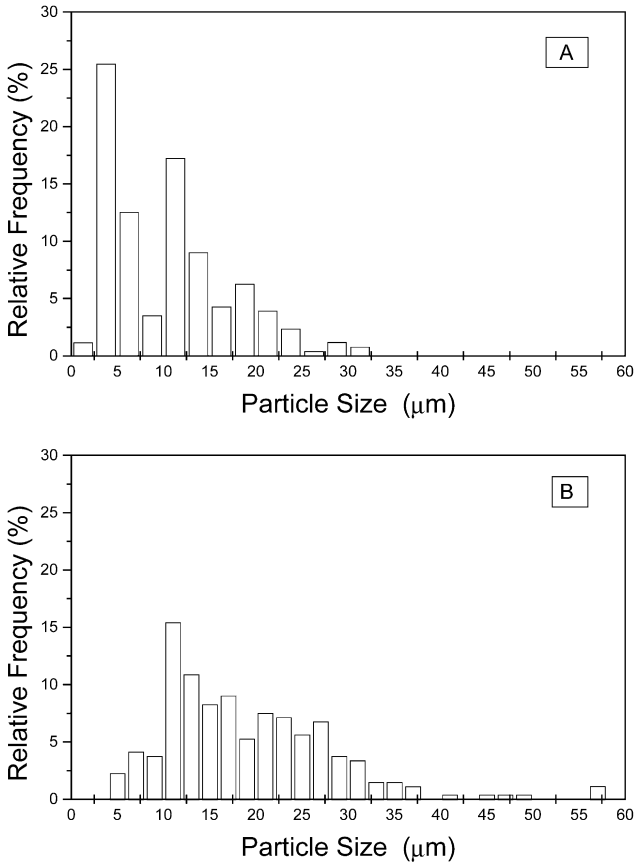

Fig. 6. Particle size distribution for particle dispersed systems: (A) resin mixture containing 3.5 wt% PFO; (B) resin mixture containing 7.0 wt% PFO.

The histograms in Fig. 6 show, in particular, that the precipitated particles become larger with increasing PFO concentration, indicating that the average diameter of the precipitated particles increases from 10 μm for systems with 3.5 wt% modified PFO to 20 μm for those containing 7.0%, while the standard deviation of the particle size increases from ±7.0 to ±10 μm.

The finding that the particle size increases with the PFO concentration is a plausible confirmation that the phase separation process is by nucleation and growth. However, it appears that there is a critical concentration of PFO above which particle growth cannot take place and that the particles will coalesce in a necklace fashion to form co-continuous domains instead of spherical aggregates, which is clearly the mechanism operating at lower concentrations [1,2]. This provides further confirmation that the particle growth mechanism cannot take place through molecular diffusion on to the surface of existing (preformed) particles, but it is likely to result from the deposition of other smaller particulate species (3–10 nm) on the surface of existing larger particles.

At higher PFO content, conditions which do not permit the formation of a particle dispersed microstructure, all properties derived from large deformation measurements, such as strength, toughness and hardness, are very similar to those obtained from systems with an IPN morphology (see Figs. 2 and 3 and Table 2).

Even at these concentrations, where there are no large particles present, the features of dynamic mechanical spectra are consistent with those of typical particle dispersed systems, except for the magnitude of the dispersions below T_g (compare, for instance, Fig. 7). The difference in the geometric organisation of the primary (preformed) particle, therefore, makes very little difference to the overall feature of the mechanical spectra, which is in concordance with the model for the aggregated nature of particles for all pre-reacted systems, spherical aggregates at low PFO concentrations and necklace co-continuous interwoven agglomerates at higher PFO contents.

It is informative to note that for particle dispersed systems there are no distinct character differences between the PFO modified systems and the those of the parent epoxy resin, other than a small discrepancy in T_g and the very minor spectral dissimilarities at lower temperatures.

The very flexible nature of the perfluoroether segments in

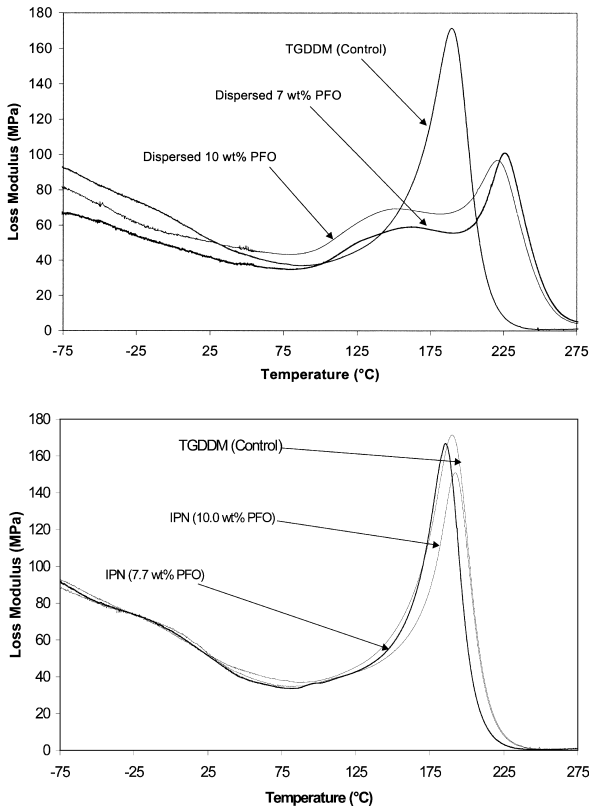

Fig. 7. (i) Dynamic mechanical spectra for particle dispersed systems. (ii) Dynamic mechanical spectra for IPN systems.

the modifier appear to have been completely offset by the rigidifying effect of the attached 'chlorendate' units. It is possible that ester exchange reactions between the MNA hardner and the adjacent 'caprolactate' units may have also contributed to suppress the plasticising effects of the perfluoroether segments and may well constitute the only plausible explanation for the features of the dynamic mechanical spectra.

Owing to the relatively low reactivity of anhydride hardners, any residual species may diffuse into the perfluoroether containing phase, particularly during post-curing, to cause the suggested ester exchange reactions. (Further work is planned to elucidate the chemical composition of the two phases.)

The features of these dynamic mechanical spectra are typical of rigid macromolecular networks, which appear to be controlled by the high functionality of the epoxy resin, and the very compact and rigid cross-linking units provided by the MNA hardner. The difference in deformational and fracture behaviour between the various systems, therefore, has to be attributed to events occurring at supranetwork and morphological levels rather than in terms of molecular dynamics. The two phases in these systems, therefore, are expected to differ from each other only with respect to the presence of perfluoroether units in the network.

The spectra of IPN systems are typical of highly interspersed heterogeneous mixtures of glassy polymers, comprising two loss-modulus peaks. The interesting feature of these IPN systems is the glassy nature of the two phases with a difference in T_g of about 75 K. Furthermore the two loss modulus peaks in the dynamic mechanical spectra are respectively below and just above the glass transition temperature of the monophase, unmodified, epoxy resin system. It has already been established that the curing kinetics of epoxy resins are affected considerably by the presence of the acid functionalised perfluoroether oligomers [4], and although in previous work it has not been possible to follow the reaction kinetics for the formation of each individual phase, it is plausible that the lower T_g of the minor phase, could be associated with a plasticisation effect by the perfluoroether units. Such a deduction can be made from the realisation that the network of this phase develops at a faster rate, due to the higher reactivity imposed by the presence of the acid functionality in modifier used for toughness enhancement [13,14]. This would cause, therefore, the PFO based minor phase to separate out earlier as a loose gel, which would then entrap the epoxy-rich major phase, forcing it form a network under restricted chain mobility. As a consequence, the cross-linking reactions in the major epoxy phase would be largely controlled by a diffusion mechanism which is responsible for the formation of a tighter, and possibly, more uniform network (see later).

The data obtained from the nanoindentation tests, presented in Table 2, show that for IPN systems there is only a slight reduction in hardness at PFO concentrations up to 7 wt% and a much larger reduction when the PFO concentration is increased to 10 wt%. One notes, in any case, that the variation in hardness over the 2 mm^2 area is negligible in comparison to the overall change in hardness values recorded with increasing perfluoroether content.

The data in Table 2 for the particle dispersed systems reveal the following features:

(a) The hardness values are uniform across the area examined only for the case of the monophase (control) epoxy resin and for the co-continuous dispersed morphology (corresponding to a 10 wt% PFO). The presence of some softer particles is revealed even at concentrations as low as 2 wt% PFO.
(b) At PFO concentrations greater than 2% the number of softer particles per unit area increases rapidly. It is noteworthy that while the hardness of the rigid, epoxy phase, remains practically constant as long as two distinct microphases are present (up to 7.5 wt%), the average hardness of the softer phase decreases and is accompanied by a widening spread of the recorded values. The latter is undoubtedly a reflection of the nature of the test as the indentor is expected to impinge in different parts of a given particle. Towards the edge of a particle, the measurements are expected to involve an increasing contribution from the surrounding matrix.
(c) At 10% PFO concentration the hardness is very uniform across the entire area examined (100 measurements) with

values only slightly higher than those recorded for the soft particles at low concentrations. It is to be remarked that the values are similar to those recorded for IPN systems at comparable concentrations.

It is worth noting that, in all cases, about 80% of the imposed indentation does not recover after removal of the load. The extent of plasticity recorded in the indentation of dispersed particles was only slightly higher than for the surrounding epoxide matrix or the unmodified epoxy resin.

These observations are not only useful for the understanding of the fracture behaviour of the materials examined, but also provide a basis for the rational interpretation for the manner in which phase separation takes place in the two systems.

It is expected that phase separation for the IPN systems take place by a spinodal decomposition through branching and cross-linking reactions). This results in sinusoidal fluctuations of composition. The one containing the perfluoroether component, owing to the presence of carboxylic acid groups, reacts much faster with the epoxy resin and is expected, therefore, to separate very readily from the surrounding binary mixture of epoxy resin and MNA hardner. The inability of the gel so produced to convert into particles, therefore, prevents also the surrounding mixture to precipitate out in the shape of particles during the subsequent cross-linking reactions, giving rise to the formation of co-continuous phases [15,16]. While the size of the domains is expected to be established at the time the IPN structured gel is produced, some diffusion of free reactive species, particularly the more mobile MNA, across the boundaries of the two phase undoubtedly takes place during the course of the curing and subsequent postcuring schedule, affecting the final chemical composition and properties of the material, as mentioned earlier.

The particulate nature of the PFO containing phase in the pre-reacted formulations, on the other hand, is due to the formation of very high molecular weight linear species which precipitate out very soon after the MNA hardner is added and much before the surrounding resin mixture reaches its gelation conditions. The absence of a substantial number of cross-links in the precipitated phase will allow it to assume a particulate geometry since the surface energy and kinetics requirements can be easily met due low viscosity of the unreacted surrounding medium. Diffusion of the very mobile MNA species into the particles is, again, expected to take place in the subsequent curing and post-curing steps.

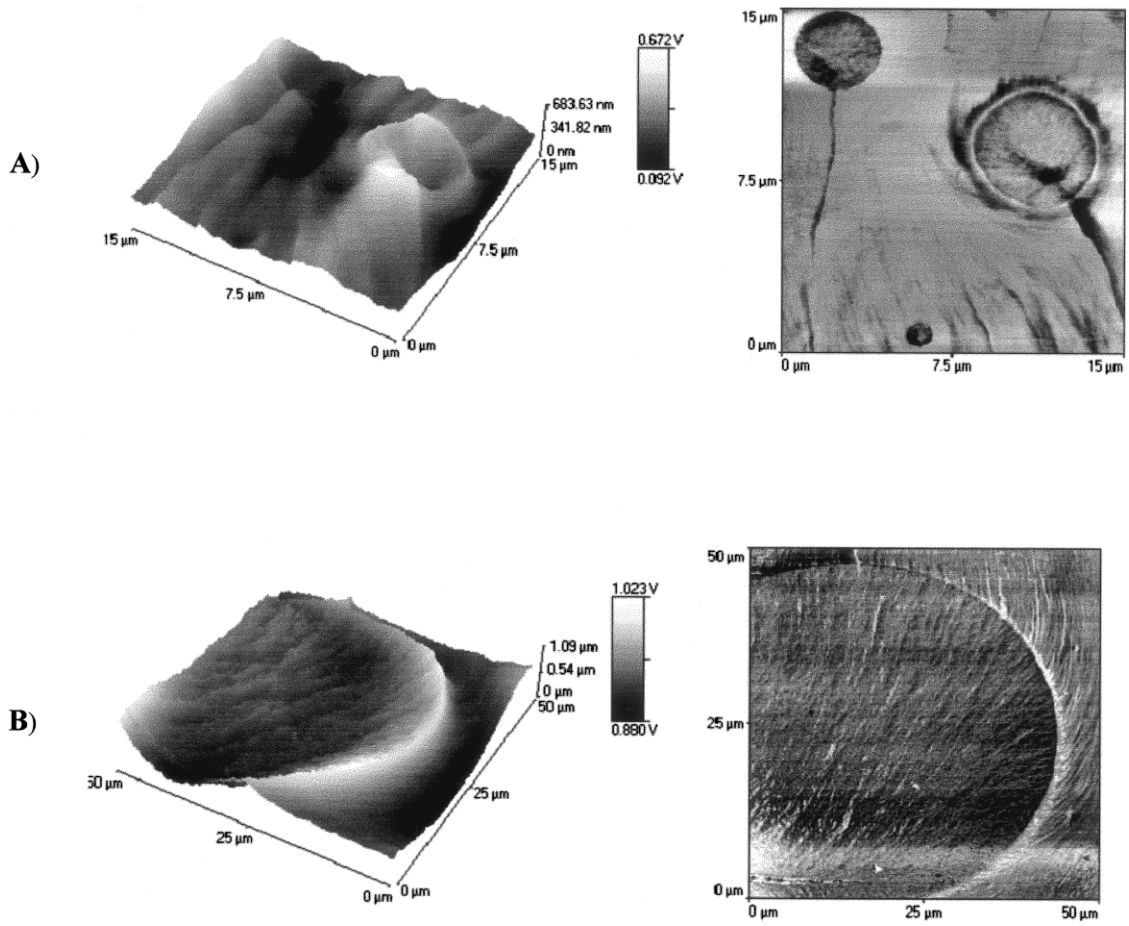

Fig. 8. AFM topography images, obtained in the 'tapping' mode, for particle dispersed systems: (A) 3.5 wt% PFO; (B) 7.0 wt% PFO.

From a close examination of the hardness data one can see a strong correlation between specific structure details with fracture toughness results in Fig. 3(i) and (ii). These indicate that the appreciable increase in fracture toughness coincides with the formation of softer particles.

One notes, furthermore, that the reduction in the rate of increase in fracture toughness, with amount of PFO used in the formulation, takes place at concentration levels where either the number of low hardness readings becomes greater than 14 per hundred (particle-dispersed systems) or the overall hardness drops to below the value of 300 MPa from the original value of 325 MPa for the unmodified resin. In contrast to this, it is noted that no direct correlation can be found between fracture toughness and yield strength data. At low PFO concentrations, for instance, the yield strength of IPN systems is even lower than for those with a particle-dispersed morphology.

The dependence of fracture toughness on local plasticity, rather than overall bulk yielding, is clearly illustrated also by the AFM micrographs in Fig. 8. These reveal the occurrence of plastic deformations within the softer particles and in the surrounding matrix. Highly localised plastic deformations are also evident at high PFO contents for both systems, where there is phase continuity at microscopic level, see Fig. 9. These show that the domain size for IPN systems is considerably smaller than for equivalent systems produced with the pre-reaction procedure. There appear to be also a difference with respect to the topography of the fractured surfaces, fibrillar for IPN systems and lamellar for those produced as for the particle dispersed procedure.

Such fine details of localised plastic deformation are not discernible, however, in the images produced by SEM, thereby placing a great reliance on AFM examinations to characterise the topography of the surfaces of these types of heterogeneous polymers.

4. Conclusions

The main conclusions that can be drawn from this study are as follows:

1. For systems prepared by pre-reacting the epoxy resin with the perfluoroether oligomer a particle-dispersed morphology is obtained only for modifier concentration

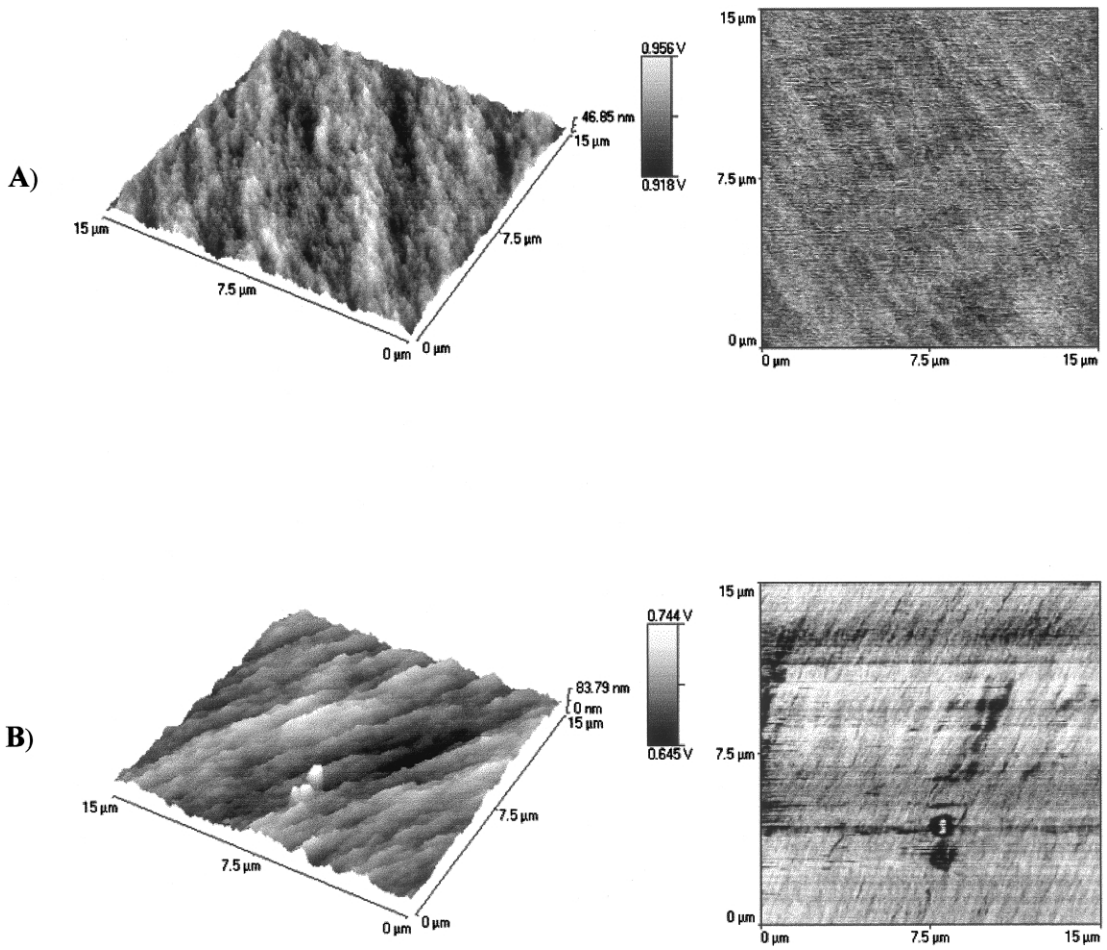

Fig. 9. AFM topography images obtained in the tapping mode, for cured resin mixtures containing 10 wt% PFO; (A) IPN systems; (B) produced as for particle-dispersed systems.

less than 10 wt%. At concentrations higher than 10 wt% the primary particles are susceptible to percolation type of interactions during particle growth, which gives rise to the formation of a co-continuous morphology.

2. Systems with a particle dispersed morphology exhibit the expected increase in toughness at much lower perfluoroether concentrations than corresponding IPN systems. Both systems give similar level of toughness enhancement at concentrations greater than 10 wt% PFO.
3. The enhancement in fracture toughness can be more closely related to local plastic deformations, resulting from the two-phase morphology, than the bulk yield strength of the material.

References

[1] Mascia L, Zitouni F, Tonelli C. J Appl Polym Sci 1994;51:995.
[2] Mascia L, Zitouni F, Tonelli C. Polym Engng Sci 1995;35:1069.
[3] Martuscelli E, Musto P, Ragosta G, Riva F, Mascia L. J Mater Sci 2000;35:3719.
[4] Musto P, Martuscelli E, Ragosta G, Mascia L. Polymer 2001;42:5189.
[5] Yamanaka K, Inoue T. J Mater Sci 1990;25:241.
[6] Kunz SC, Sayre JA, Assink RA. Polymer 1982;23:1897.
[7] Warrik EL, Pierce OR, Polmanteer KE, Saam JC. Rubb Chem Technol 1979;52:437.
[8] Kubotera K, Yee AF. ANTEC '93, New Orleans, Lousiana; 9–13 May 1993. p. 3290.
[9] Bucknall CB, Partridge KI. Polymer 1983;24:639.
[10] Raghava RS. J Polym Sci-Polym Phys 1987;25:1017.
[11] Brow F, Srawley J. ASTMspec. Tech. Publ. No.510; 1966. p. 13.
[12] Plati E, Williams JG. Polym Engng Sci 1975;15:470.
[13] Wise CW, Cook WD, Goodwin AA. Polymer 2000;41:4625.
[14] Jenninger W, Schawe JEK, Allig I. Polymer 2000;41:1577.
[15] Innue T. Prog Polym Sci 1995;20:119.
[16] Bansil R, Liao C. Trends Polym Sci 1997;5:146.